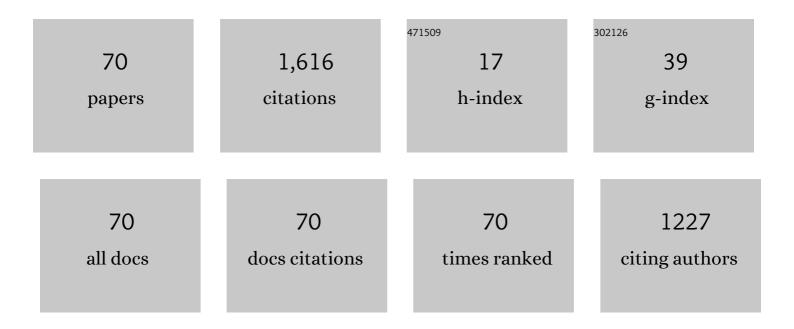
## David D Allred

List of Publications by Year in descending order

Source: https://exaly.com/author-pdf/556864/publications.pdf Version: 2024-02-01



#	Article	IF	CITATIONS
1	Superconductivity at 155 K. Physical Review Letters, 1987, 58, 2579-2581.	7.8	291
2	Profiling hydrogen in materials using ion beams. Nuclear Instruments & Methods, 1978, 149, 19-39.	1.2	198
3	The Extreme Ultraviolet Imager Investigation for the IMAGE Mission. Space Science Reviews, 2000, 91, 197-242.	8.1	155
4	Optical properties and structure of amorphous silicon films prepared by CVD. Solar Energy Materials and Solar Cells, 1979, 1, 11-27.	0.4	124
5	Chemically vapor-deposited ZrB2 as a selective solar absorber. Thin Solid Films, 1981, 83, 393-398.	1.8	85
6	The use of nuclear reactions and SIMS for quantitative depth profiling of hydrogen in amorphous silicon. Applied Physics Letters, 1977, 31, 582-585.	3.3	65
7	Determination of the Insulation Gap of Uranium Oxides by Spectroscopic Ellipsometry and Density Functional Theory. Journal of Physical Chemistry C, 2013, 117, 16540-16551.	3.1	57
8	Photoluminescence and absorption studies of defects in CdTe andZnxCd1â^'xTe crystals. Physical Review B, 1993, 47, 13363-13369.	3.2	50
9	The application of nuclear reactions for quantitative hydrogen analysis in a variety of different materials problems. Nuclear Instruments & Methods, 1978, 149, 9-18.	1.2	45
10	Stabilized CVD amorphous silicon for high temperature photothermal solar energy conversion. Solar Energy Materials and Solar Cells, 1979, 2, 107-124.	0.4	45
11	Low-frequency feature in the first-order Raman spectrum of amorphous carbon. Physical Review B, 1993, 47, 6119-6121.	3.2	37
12	Eliminating carbon contamination on oxidized Si surfaces using a VUV excimer lamp. Thin Solid Films, 2008, 517, 1011-1015.	1.8	32
13	The Extreme Ultraviolet Imager Investigation for the Image Mission. , 2000, , 197-242.		32
14	Retarding crystallization of CVD amorphous silicon by alloying. Journal of Non-Crystalline Solids, 1980, 35-36, 213-218.	3.1	31
15	Deconvolution of the Raman spectrum of amorphous carbon. Journal of Raman Spectroscopy, 1995, 26, 1039-1043.	2.5	24
16	Raman scattering and x-ray diffraction characterization of amorphous semiconductor multilayer interfaces. Journal of Materials Research, 1986, 1, 468-475.	2.6	19
17	Structural phase transition andTcdistribution in Hf-doped LaMnO3investigated using perturbed-angular-correlation spectroscopy. Physical Review B, 1996, 54, R3679-R3682.	3.2	19
18	Measured optical constants of copper from 10 nm to 35 nm. Optics Express, 2009, 17, 23873.	3.4	19

DAVID D ALLRED

#	Article	IF	CITATIONS
19	Emitted current instability from silicon field emission emitters due to sputtering by residual gas ions. Journal of Vacuum Science and Technology A: Vacuum, Surfaces and Films, 1994, 12, 2581-2585.	2.1	17
20	Characterization of Chemical Speciation in Ultrathin Uranium Oxide Layered Films. Analytical Chemistry, 2012, 84, 10380-10387.	6.5	16
21	Effect of iron catalyst thickness on vertically aligned carbon nanotube forest straightness for CNT-MEMS. Journal of Micromechanics and Microengineering, 2012, 22, 055004.	2.6	16
22	Raman spectroscopic study of the formation of tâ€MoSi2 from Mo/Si multilayers. Journal of Vacuum Science and Technology A: Vacuum, Surfaces and Films, 1994, 12, 1535-1541.	2.1	15
23	Hydrogen concentration profiles in quartz determined by a nuclear reaction technique. Physics and Chemistry of Minerals, 1978, 3, 199-211.	0.8	14
24	Mesostructure of photoluminescent porous silicon. Journal of Vacuum Science and Technology A: Vacuum, Surfaces and Films, 1994, 12, 2565-2571.	2.1	14
25	Characterization of asâ€prepared and annealed W/C multilayer thin films. Journal of Vacuum Science and Technology A: Vacuum, Surfaces and Films, 1992, 10, 145-151.	2.1	13
26	Spectrally selective surfaces by chemical vapor deposition. Solar Energy Materials and Solar Cells, 1985, 12, 87-129.	0.4	12
27	Waterjet cutting of crossâ€linked glass. Journal of Vacuum Science and Technology A: Vacuum, Surfaces and Films, 1995, 13, 136-139.	2.1	12
28	Determining indices of refraction for ThO2 thin films sputtered under different bias voltages from 1.2 to 6.5ÂeV by spectroscopic ellipsometry. Thin Solid Films, 2006, 515, 847-853.	1.8	12
29	A comparison of uranium oxide and nickle as single-layer reflectors from 2.7 to 11.6 nm. , 2004, , .		9
30	<title>Dual-function EUV multilayer mirrors for the IMAGE mission</title> ., 1999, 3767, 280.		8
31	Highly Reflective Uranium Mirrors for Astrophysics Applications. , 2002, , .		8
32	High-Aspect-Ratio Metal Microfabrication by Nickel Electroplating of Patterned Carbon Nanotube Forests. Journal of Microelectromechanical Systems, 2015, 24, 1331-1337.	2.5	8
33	PECVD growth of Six:Ge1â^'x films for high speed devices and MEMS. Journal of Non-Crystalline Solids, 2006, 352, 1272-1274.	3.1	7
34	Polymer molded templates for nanostructured amorphous silicon photovoltaics. Journal of Vacuum Science and Technology A: Vacuum, Surfaces and Films, 2011, 29, .	2.1	7
35	β-Delayed Proton Decay ofC9. Physical Review C, 1972, 6, 373-375.	2.9	6
36	The effect of oxygen on the structure of annealed w/c multilayer thin films. Solid State Communications, 1991, 79, 205-207.	1.9	6

DAVID D ALLRED

#	Article	IF	CITATIONS
37	Characterization of optical constants for uranium from 10 to 47 nm. Applied Optics, 2010, 49, 1581.	2.1	6
38	Formation of solid thorium monoxide at near-ambient conditions as observed by neutron reflectometry and interpreted by screened hybrid functional calculations. Journal of Nuclear Materials, 2017, 487, 288-296.	2.7	6
39	Raman Spectroscopic Analysis of Mo/Si Multilayers. Journal of X-Ray Science and Technology, 1992, 3, 222-228.	1.0	5
40	Thorium-Based Thin Films as Highly Reflective Mirrors in the EUV. Materials Research Society Symposia Proceedings, 2005, 893, 1.	0.1	5
41	An inexpensive high-temperature optical fiber thermometer. Journal of Quantitative Spectroscopy and Radiative Transfer, 2017, 187, 358-363.	2.3	5
42	Oxide structure of air-passivated U-6Nb alloy thin films. Journal of Nuclear Materials, 2020, 539, 152356.	2.7	5
43	Y <sub>2</sub> O <sub>3</sub> optical constants between 5 nm and 50 nm. Optics Express, 2019, 27, 3324.	3.4	5
44	Diffuse absorbing beryllium coatings produced by magnetron sputtering. , 1990, 1331, 170.		4
45	Using thin film stress to produce precision, figured X-ray optics. Thin Solid Films, 1992, 220, 284-288.	1.8	4
46	Optical properties and application of uranium-based thin films for the extreme ultraviolet and soft x-ray region. , 2004, 5538, 107.		4
47	Determining ruthenium's optical constants in the spectral range 11-14 nm. , 2004, 5538, 84.		4
48	Oxidation of aluminum thin films protected by ultrathin MgF2 layers measured using spectroscopic ellipsometry and X-ray photoelectron spectroscopy. OSA Continuum, 2021, 4, 879.	1.8	4
49	<title>Optical constants of sputtered U and a-Si at 30.4 and 58.4 nm</title> . , 1999, 3767, 288.		3
50	Uranium Oxide as a Highly Reflective Coating from 100–400 eV. AIP Conference Proceedings, 2004, , .	0.4	3
51	Understanding DC-bias sputtered thorium oxide thin films useful in EUV optics. , 2006, , .		3
52	Thorium dioxide thin films in the extreme ultraviolet. , 2006, 6317, 262.		3
53	Extreme-ultraviolet polarimeter utilizing laser-generated high-order harmonics. Review of Scientific Instruments, 2008, 79, 103108.	1.3	3
54	Optical constants of evaporated amorphous zinc arsenide (Zn <sub>3</sub> As <sub>2</sub> ) via spectroscopic ellipsometry. Optical Materials Express, 2019, 9, 4677.	3.0	3

DAVID D ALLRED

0

#	Article	IF	CITATIONS
55	Characterization of Metal/Carbon Multilayers by Raman Spectroscopy. Materials Research Society Symposia Proceedings, 1989, 160, 605.	0.1	2
56	Observation of beam-induced changes in the polarization of Balmer-α radiation emitted following beam–tilted-foil transmission. Physical Review A, 1995, 52, 4631-4639.	2.5	2
57	Raman spectrographic system for quantitative analysis of isotopic hydrogen mixtures for muon catalysis experiments. Hyperfine Interactions, 1996, 101-102, 695-698.	0.5	2
58	A rotating electrochemical cell to prepare porous silicon with different surface structures. Thin Solid Films, 1999, 338, 100-104.	1.8	2
59	Using ellipsometry and x-ray photoelectron spectroscopy for real-time monitoring of the oxidation of aluminum mirrors protected by ultrathin MgF2 layers. , 2019, , .		2
60	The Hydrogen Content of Multicomponent Amorphous Silicon Alloys by 19F Nuclear Reaction Analysis. IEEE Transactions on Nuclear Science, 1981, 28, 1838-1840.	2.0	1
61	Diode properties of nanotube networks. Thin Solid Films, 2010, 518, 5014-5017.	1.8	1
62	Progress towards adding EUV reflectance to broadband Al mirrors for space-based observatories. , 2017, , .		1
63	<title>Transmittances of thin polymer films and their suitability as a supportive substrate for a soft&lt;br&gt;x-ray solar filter</title> . , 1991, 1549, 147.		0
64	Multilayer phase diffraction gratings modeled as a structure in three dimensions. , 1993, 1742, 476.		0
65	<title>X-ray diode using a silicon field-emission photocathode</title> . , 1993, , .		0
66	Use of Raman spectroscopy in characterizing soft x-ray multilayers: tools in understanding structure and interfaces. , 1993, , .		0
67	Characterization Of Boron Films Prepared By Chemical Vapor Deposition And Their Application In X-Ray Imaging. Materials Research Society Symposia Proceedings, 1993, 306, 189.	0.1	0
68	Intermediate Martian Atmospheric Study and Demonstrator. , 2006, , .		0
69	Reflecting at 30.4 and Antireflecting at 58.4 nm. , 2007, , .		0

70 Extreme-ultraviolet polarimetry with laser-generated high-order harmonics. , 2008, , .